Austin Journal of Bioorganic & Organic Chemistry

Open Access

Austin Publishing Group

Research Article

Quinoline Derivatives: Design and Synthesis as a Potential COVID-19 Protease Inhibitor

Mani R* and Ranjith WAC

Centre for Molecular and Nanomedical Sciences, International Research Centre, Sathyabama Institute of Science and Technology (Deemed to be University), India

***Corresponding author: Rajeshekar Mani**

Centre for Molecular and Nanomedical Sciences, International Research Centre, Sathyabama Institute of Science and Technology (Deemed to be University), Chennai - 600 119, India

Received: November 21, 2022; **Accepted:** January 30, 2023**; Published:** February 06, 2023

Abstract

A multicomponent one-pot reaction involving Phenylacetylene, 4-Aminofluorescein and aromatic aldehydes using Cu (I) as a catalyst is described, which provides an efficient and practical route to synthesize quinoline in good yield. The compound was analyzed for its potential to act on 3C-like proteinase using *in silico* docking studies, 4b and 4c showed a docking score of -8.2 kcal/mol (2 hydrogen bonds) and -8.1 kcal/mol (2 hydrogen bonds) respectively for monomer of 3C-like protease, and -8.88 kcal/mol (3 hydrogen bonds) and -8.9 kcal/mol (4 hydrogen bonds) respectively for dimer of 3C-like protease. These provide an insight of using Quinolines as a potential drug to target COVID 19 protein target 3C-like protease.

Keywords: Aminofluorescein; Quinoline; One-Pot Reaction; Phenylacetylene; COVID 19

Introduction

An outbreak of a series of acute respiratory illness caused by a novel coronavirus, SARS-CoV-2, caused a global threat in 2020. The World Health Organization (WHO) named the disease "COVID-19" and declared it as a world health emergency pandemic. Quinolines play an important role in organic chemistry. They are important structural motifs that exist in numerous natural products are shown in (Figure 1) [1-3]. Quinolines are heterocyclic molecules composed off used benzene and pyridine rings. The quinolines can possess various biological activities, including antiproliferative [4], antiviral [5], antibacterial [6], antifungal [7], anti-inflammatory [8], and antiparasitic [9]. Members of the quinoline family, such as chloroquine and hydroxychloroquine, have shown antiviral activity against several viruses, such as coronaviruses [5], human immunodeficiency virus [10], and respiratory syncytial virus [11]. Concerning Flavivirus, quinoline derivatives have proved active against the Hepatitis C virus [12], West Nile virus [13], Japanese Encephalitis virus [14], Zika virus [15], and dengue virus. It also found wide utility as efficient organo-catalysts and used as a ligand for the preparation of phosphorescent complexes. They are useful tools for the highly enantio selective syntheses of chiral molecules [16,17].

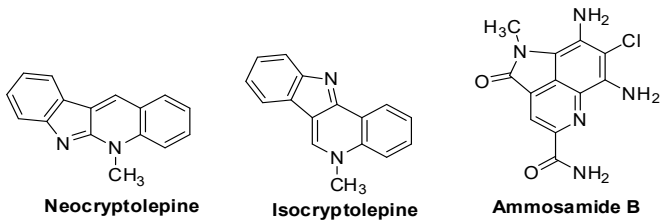

Figure 1: Structures of quinoline ring containing natural products.

Among these Multicomponent Reactions (MCRs) provides easy access to the preparation of quinoline derivatives, because Multicomponent Reactions (MCRs) have emerged as bond-forming efficient tools in medicinal chemistry [18,19]. All these procedures are through strong acid/metal-catalyzed sequential intermolecular addition of alkynes onto imines and subsequent intramolecular ring closure by arylation. The quinoline core in both biological and chemical fields, new direct approaches remain highly valuable to the contemporary collection of synthetic methods [20,21]. The study shows that most of the one-pot reaction involves amine, aldehyde, and acetylene moieties to synthesize quinoline derivatives [22]. In the context of our studies in the area of MCRs, we would like to report an efficient

Citation: Mani R, Ranjith WAC. Quinoline Derivatives: Design and Synthesis as a Potential COVID-19 Protease Inhibitor. Austin J Bioorg & Org Chem. 2023; 2(1): 1005.

approach for the one-pot synthesis of quinolone and target the protein of COVID 19.

Experimental Section

General Methods

4-Aminofluorescein, Aldehydes, Phenylacetylene, Copper chloride and other solvents were obtained from SRL, Chennai, Tamil Nadu, India. Column chromatography was performed on Silica Gel (100-200 mesh). Melting points were measured on a Sigma micro melting point apparatus and are uncorrected. NMR spectra were recorded on Bruker DRX 300 MHz in $CDCl_3$ or DMSO-d_6 at the University of Madras (Chennai, Tamil Nadu, India). TMS was used as the internal standard (δ = 0.00 ppm) and all the *J* values are given in hertz. Elemental analyses were performed using Perkin-Elmer 2400 elemental analyzer.

General Procedure for the Synthesis of Quinoline (4a-e)

To a solution of the aldehydes (**1a-e**, 1.0 mmol), 4-Aminofluorescein (**2**, 1.0 mmol), Phenylacetylene (**3**, 1.0 mmol) and dry THF (10 mL) were added copper chloride (0.3 mmol). After stirring at 80ºC (oil bath temperature) for a given period of time, the reaction mixture was evaporated under reduced pressure and extracted by DCM-water. The DCM layer was dried over anhyd. Na_2SO_4 and concentrated to dryness. The product was further purified by flash column chromatography.

Physicochemical and spectral data for 2-(4-chlorophenyl)-3',6'-dihydroxy-4-phenyl-8H-spiro[furo[3,4-g]quinoline-6,9'-xanthen]-8-one (4a): A mixture of 4-Chlorobenzaldehyde (**1a**, 0.14 g, 1.0 mmol), 4-Aminofluorescein (**2**, 0.34 g, 1.0 mmol), Phenylacetylene (**3**, 0.10 g, 1.0 mmol) and CuCl (0.07 g, 0.3 mmol) in 10 mL of THF afforded compound **4a** as an pale yellow solid (0.41 g, 73%); mp 152-154ºC; $[\alpha]_D^{31}$ + 58.8 (*c* 0.1, $CHCl_3$); ^{1}H NMR: ($CDCl_3$, 300 MHz): δ 6.74 (d, 2H, *J* = 8.4 Hz, Ar-H), 6.77 (d, 1H, *J* = 8.4 Hz, Ar-H), 6.98 (t, 2H, *J* = 7.8 Hz, Ar-H), 7.08 (t, 2H, *J* = 9.9 Hz, Ar-H), 7.32 (t, 1H, *J* = 8.0 Hz, Ar-H), 7.58 (q, 4H, *J* = 7.5 Hz, Ar-H), 7.70 (d, 3H, *J* = 6.8 Hz, Ar-H), 8.09 (q, 1H, *J* = 8.5 Hz, Ar-H), 8.23 (s, 2H, Ar-OH), 8.25 (d, 2H, *J* = 7.8 Hz, Ar-H). ^{13}C NMR: ($CDCl_3$, 75 MHz): δ 82.8, 110.2, 116.4, 117.9, 118.4, 119.4, 124.2, 125.3, 125.6, 126.1, 128.4, 128.8, 128.9, 129.0, 130.2, 130.3, 130.4, 130.6, 133.9, 134.3, 135.4, 149.8, 150.2, 150.6, 150.8, 152.8, 164.5, 169.1, Anal. Calcd for $C_{35}H_{20}ClNO_5$: C, 73.75; H, 3.54; N, 2.46. Found: C, 73.76; H, 3.52; N, 2.44.

Physicochemical and spectral data for 2-(4-bromophenyl)-3',6'-dihydroxy-4-phenyl-8H-spiro[furo[3,4-g]quinoline-6,9'-xanthen]-8-one (4b): A mixture of 4-Bromobenzaldehyde (**1b**, 0.18 g, 1.0 mmol), 4-Aminofluorescein (**2**, 0.34 g, 1.0 mmol), Phenylacetylene (**3**, 0.10 g, 1.0 mmol) and CuCl (0.07 g, 0.3 mmol) in 10 mL of THF afforded compound **4b** as an pale yellow solid (0.43 g, 70%); $[\alpha]_D^{31}$ + 68.2 (*c* 0.1, $CHCl_3$); ^{1}H NMR: ($CDCl_3$, 300 MHz): δ 6.72 (d, 2H, *J* = 7.2 Hz, Ar-H), 6.75 (d, 1H, *J* = 8.4 Hz, Ar-H), 6.95 (t, 2H, *J* = 7.2 Hz, Ar-H), 7.09 (t, 2H, *J* = 7.2 Hz, Ar-H), 7.35 (d, 1H, *J* = 7.4 Hz, Ar-H), 7.55 (q, 2H, *J* = 7.5 Hz, Ar-H), 7.62 (d, 2H, *J* = 7.5 Hz, Ar-H), 7.72 (d, 3H, *J* = 6.8 Hz, Ar-H), 8.12 (q, 1H, *J* = 7.5 Hz, Ar-H), 8.22 (s, 2H, Ar-OH), 8.28 (d, 2H, *J* = 7.5 Hz, Ar-H). ^{13}C NMR: ($CDCl_3$, 75 MHz): δ 82.6, 110.4, 116.6, 117.5, 118.2, 119.5, 124.4, 125.5, 125.8, 126.7, 128.2, 128.5, 128.8, 129.6, 130.1, 130.3, 130.5, 130.7, 133.5, 134.5, 135.4, 149.6, 150.4, 150.6, 150.8, 152.6, 164.6, 169.5, Anal. Calcd for $C_{35}H_{20}BrNO_5$: C, 68.42; H, 3.28; N, 2.28. Found: C, 68.44; H, 3.26; N, 2.26.

Physicochemical and spectral data for 2-(4-fluorophenyl)-3',6'-dihydroxy-4-phenyl-8H-spiro[furo[3,4-g]quinoline-6,9'-xanthen]-8-one (4c): A mixture of 4-Fluorobenzaldehyde (**1c**, 0.12 g, 1.0 mmol), 4-Aminofluorescein (**2**, 0.34 g, 1.0 mmol), Phenylacetylene (**3**, 0.10 g, 1.0 mmol) and CuCl (0.07 g, 0.3 mmol) in 10 mL of THF afforded compound **4c** as an pale yellow solid (0.37 g, 67%); $[\alpha]_D^{31}$ + 65.7 (*c* 0.1, $CHCl_3$); ^{1}H NMR: ($CDCl_3$, 300 MHz): δ 6.73 (d, 2H, *J* = 8.4 Hz, Ar-H), 6.78 (d, 2H, *J* = 8.4 Hz, Ar-H), 6.96 (d, 2H, *J* = 7.5 Hz, Ar-H), 7.09 (t, 2H, *J* = 7.5 Hz, Ar-H), 7.32 (d, 1H, *J* = 8.0 Hz, Ar-H), 7.58 (d, 4H, *J* = 7.2 Hz, Ar-H), 7.70 (d, 2H, *J* = 7.6 Hz, Ar-H), 8.08 (d, 1H, *J* = 8.2 Hz, Ar-H), 8.23 (s, 2H, Ar-OH), 8.25 (d, 2H, *J* = 7.2 Hz, Ar-H). ^{13}C NMR: ($CDCl_3$, 75 MHz): δ 82.5, 110.3, 116.6, 117.6, 118.4, 119.5, 124.5, 125.3, 125.8, 126.5, 128.3, 128.8, 128.9, 129.6, 130.1, 130.3, 130.4, 130.8, 133.8, 134.3, 135.6, 149.6, 150.2, 150.6, 150.8, 152.8, 164.6, 169.2. Anal. Calcd for $C_{35}H_{20}FNO_5$: C, 75.94; H, 3.64; N, 2.53. Found: C, 75.92; H, 3.66; N, 2.54.

3.2.4 Physicochemical and spectral data for 3',6'-dihydroxy-2-(4-iodophenyl)-4-phenyl-8H-spiro[furo[3,4-g]quinoline-6,9'-xanthen]-8-one (4d): A mixture of 4-Iodobenzaldehyde (**1d**, 0.23 g, 1.0 mmol), 4-Aminofluorescein (**2**, 0.34 g, 1.0 mmol), Phenylacetylene (**3**, 0.10 g, 1.0 mmol) and CuCl (0.07 g, 0.3 mmol) in 10 mL of THF afforded compound **4d** as an pale yellow solid (0.45 g, 68%); $[\alpha]_D^{31}$ + 56.8 (*c* 0.1, $CHCl_3$); ^{1}H NMR: ($CDCl_3$, 300 MHz): δ 6.75 (d, 2H, *J* = 8.4 Hz, Ar-H), 6.78 (d, 1H, *J* = 8.4 Hz, Ar-H), 6.96 (d, 2H, *J* = 7.8 Hz, Ar-H), 7.08 (d, 2H, *J* = 7.8 Hz, Ar-H), 7.32 (t, 2H, *J* = 8.0 Hz, Ar-H), 7.62 (q, 3H, *J* = 7.5 Hz, Ar-H), 7.74 (d, 3H, *J* = 7.2 Hz, Ar-H), 8.11 (q, 1H, *J* = 8.2 Hz, Ar-H), 8.25 (s, 2H, Ar-OH), 8.28 (d, 2H, *J* = 7.8 Hz, Ar-H). ^{13}C NMR: ($CDCl_3$, 75 MHz): δ 82.8, 110.5, 116.5, 117.8, 118.5, 119.6, 124.4, 125.1, 125.6, 126.5, 128.3, 128.8, 128.9, 129.5, 130.2, 130.3, 130.4, 130.6, 133.6, 134.6, 135.6, 149.7, 150.2, 150.6, 150.8, 152.7, 164.5, 169.3. Anal. Calcd for $C_{35}H_{20}INO_5$: C, 63.55; H, 3.05; N, 2.12. Found: C, 63.55; H, 3.05; N, 2.12.

Physicochemical and spectral data for 3',6'-dihydroxy-4-phenyl-2-(p-tolyl)-8H-spiro[furo[3,4-g]quinoline-6,9'-xanthen]-8-one (4e): A mixture of 4-Methylbenzaldehyde (**1e**, 0.12 g, 1.0 mmol), 4-Aminofluorescein (**2**, 0.34 g, 1.0 mmol), Phenylacetylene (**3**, 0.10 g, 1.0 mmol) and CuCl (0.07 g, 0.3 mmol) in 10 mL of THF afforded compound **4e** as an pale yellow solid (0.36 g, 66%); $[\alpha]_D^{31}$ + 62.8 (*c* 0.1, $CHCl_3$); ^{1}H NMR: ($CDCl_3$, 300 MHz): δ 2.34 (s, 3H, -CH_3), 6.75 (d, 2H, *J* = 8.4 Hz, Ar-H), 6.77 (d, 1H, *J* = 8.4 Hz, Ar-H), 6.96 (d, 2H, *J* = 7.8 Hz, Ar-H), 7.08 (t, 2H, *J* = 7.8 Hz, Ar-H), 7.38 (t, 2H, *J* = 8.0 Hz, Ar-H), 7.56 (q, 3H, *J* = 7.5 Hz, Ar-H), 7.72 (d, 3H, *J* = 6.8 Hz, Ar-H), 8.08 (d, 1H, *J* = 8.5 Hz, Ar-H), 8.23 (s, 2H, Ar-OH), 8.28 (d, 2H, *J* = 7.8 Hz, Ar-H). ^{13}C NMR: ($CDCl_3$, 75 MHz): δ 20.1, 82.5, 110.4, 116.7, 117.9, 118.6, 119.6, 124.5, 125.7, 125.7, 126.1, 128.2, 128.8, 128.9, 129.3, 130.2, 130.3, 130.4, 130.9, 133.2, 134.1, 135.4, 149.6, 150.2, 150.6, 150.8, 152.5, 164.2, 169.2. Anal. Calcd for $C_{36}H_{23}NO_5$: C, 78.68; H, 4.22; N, 2.55. Found: C, 78.66; H, 4.24; N, 2.53.

Ligand-Based Target Prediction and Molecular Docking Studies

The 3D structure of the molecule is drawn using the Discovery Studio software and was subjected to target protein prediction studies using D3 Similarity in the D3Targets-2019-nCoV server [23]. The Server uses two-dimensional and three-dimensional similarity of known molecular structure to predict target proteins for the desire/ query compounds. Further docking was performed using the D3Docking server which used Autodock Vina [24] to study the efficiency of the molecule for interaction with the 3C-like protease of COVID 19. K36 and O6K were used as control for the study.

Results and Discussion

Synthesis of Quinolines

Aldehydes (**1a-e**) and 4-Aminofluorescein (**2**) reacts with phenylacetylene (**3**) in the presence of CuCl as a catalyst in THF solvent and results in 66-73% yield of the respective quinoline (**4a-e**) as shown in (Scheme 1). The ^{1}H NMR spectra of the quinoline exhibit signals for the aromatic ring of the quinoline core structure in the region of 8.22-6.98 ppm. However, the aromatic carbons in the ^{13}C NMR spectrum corresponding to the quinoline core structure resonate in the region of 158.1-110.2 ppm, which provides evidence for the quinoline over the possible fluorescein-amine. All these observations provide clear support for the formation of the 2,4-disubstituted quinoline. Structure of reaction time and product yields are given in (Table 1).

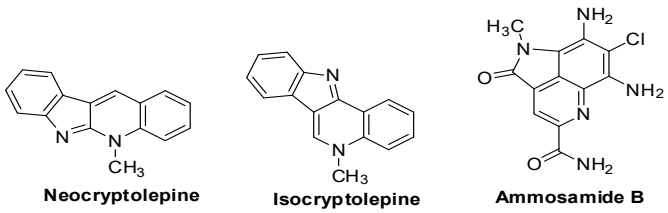

Scheme 1: Synthesis of quinolines.

Table 1: Structure of reaction time and product yields.

S. No	R	Time (h)	Yield (%)
1	Cl (**4a**)	8	73
2	Br (**4b**)	8	70
3	F (**4c**)	8	67
4	I (**4d**)	8	68
5	Me (**4e**)	8	66

The first A^3 coupling approach for quinoline synthesis was described by Rajasekar et al. in the presence of catalyst CuCl in 2014 [24]. The A^3 coupled product propargylamine **5** underwent a Cu-mediated allenyl isomerization (**6**), followed by a intramolecular cyclization and dehydrogenative oxidation to accomplish quinoline **4a-e** are shown in (Scheme 2).

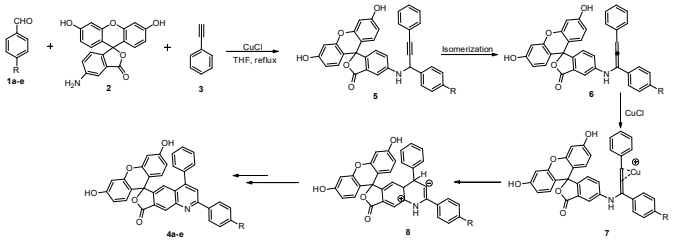

Scheme 2: First A^3 coupling approach for quinoline synthesis.

Target Prediction using D3 Similarity

D3Similarity is based on the two-dimensional and three-dimensional similarity of molecular structure. The target proteins are predicted based on the active compounds already available from experimental studies, followed by virtual screening via 2D and 3D similarities. The compounds showed a similarity index of 20.74 to CBMicro_032111 which is an inhibitor of 3C-like protease (Table 2). COVID 19 protein targets were primaried in the present study and the docking were performed.

Table 2: COVID 19 protein Target prediction of compounds using 3D similarity search.

Compound	Pubchem CID	Mol ID	Similarity	3D Similarity	2D Similarity	Target Name
4a	2867165	CBMicro_032111	20.74	69.64	29.77	virus: 3C-like protease
4b	2867165	CBMicro_032111	20.98	69.48	30.19	virus: 3C-like protease
4c	70673796	CHEMBL2235440	20.82	61.8	33.69	virus: 3C-like protease
4d	2867165	CBMicro_032111	20.74	69.64	29.77	virus: 3C-like protease
4e	70673796	CHEMBL2235440	21.57	61.98	0.348	virus: 3C-like protease
4a	66839793	2-(3,4-Dihydroxyphenyl)-6-(3,7-dimethylocta-2,6-dienyl)-5,7-dihydroxy-2,3-dihydrochromen-4-one	22.01	61.98	0.3221	virus: Papain-like protease
4b	66839793	2-(3,4-Dihydroxyphenyl)-6-(3,7-dimethylocta-2,6-dienyl)-5,7-dihydroxy-2,3-dihydrochromen-4-one	22.01	68.34	0.3221	virus: Papain-like protease
4c	66839793	2-(3,4-Dihydroxyphenyl)-6-(3,7-dimethylocta-2,6-dienyl)-5,7-dihydroxy-2,3-dihydrochromen-4-one	22.71	68.35	0.3209	virus: Papain-like protease
4d	66839793	2-(3,4-Dihydroxyphenyl)-6-(3,7-dimethylocta-2,6-dienyl)-5,7-dihydroxy-2,3-dihydrochromen-4-one	21.91	70.76	0.3209	virus: Papain-like protease
4e	66839793	2-(3,4-Dihydroxyphenyl)-6-(3,7-dimethylocta-2,6-dienyl)-5,7-dihydroxy-2,3-dihydrochromen-4-one	22.63	68.26	0.332	virus: Papain-like protease

Docking and Interaction of Synthesized Componds against 3C-like Protease

Docking studies were carried out between the protein and the ligand in D3Docking server. The docking studies were performed against the dimer and monomer of 3C-like protease. CYS A:145, HIS A:163, HIS A:164, GLU A:166, HIS A:41, MET A:49, TYR A:54, PHE A:140, LEU A:141, ASN A:142, GLY A:143, SER A:144, MET A:165, HIS A:172, ASP A:187, GLN A:189 are the active site amino acid of the monomer of 3C-like protease, similarly THR A:26, HIS A:41, MET A:49, PHE A:140, LEU A:141, ASN A:142, GLY A:143, SER A:144, CYS A:145, HIS A:163, HIS A:164, MET A:165, GLU A:166, HIS A:172, ASP A:187, GLN A:189 are the active site residues of dimer of 3C-like protease. The docking score for 4b and 4c of -8.2 kcal/mol and -8.1 kcal/mol respectively for monomer of 3C-like protease, and -8.88 kcal/mol and -8.9 kcal/mol respectively for dimer of 3C-like protease (Table 3). The molecular interactions shows 4b and 4c has 2 hydrogen bonds each comparitivly less when compared to K36 (8) and O6K (5) for 3C-like protease monomer (Figure 2). The in-

teraction of 4b and 4c with 3C-like protease dimer also showed 3 and 4 hydrogen bonds when compared to K36 and O6K which showed 6 hydrogen bond. Similar hydrophobic interactions were observed in all the interactions (Figure 3).

Table 3: Hydrogen bond and hydrophobic interaction between compounds and 3C-like protease.

Compound	3C-like protease monomer	3C-like protease dimer	3C-like protease monomer (Interactions)				3C-like protease dimer (Interactions)			
4a	-6.6	-6.8	Hydrophobic	41A	HIS	3.28	Hydrophobic	25A	THR	2.82
			Hydrophobic	47A	GLU	3.97	Hydrophobic	27A	LEU	3.47
			Hydrophobic	141A	LEU	3.81	Hydrophobic	166A	GLU	3.92
			Hydrophobic	166A	GLU	3.9	Hydrophobic	168A	PRO	2.94
			Hydrophobic	187A	ASP	3.71	Hydrogen Bond	1B	SER	2.89
			π-Stacking 41A	HIS		4.86	Hydrogen Bond	47A	GLU	2.95
							Hydrogen Bond	166A	GLU	2.25
							Hydrogen Bond	166A	GLU	1.8
							Hydrogen Bond	189A	GLN	2.71
4b	-8.2	-8.8	Hydrophobic	140A	PHE	3.81	Hydrophobic	140A	PHE	3.8
			Hydrophobic	141A	LEU	3.87	Hydrophobic	165A	MET	3.87
			Hydrophobic	166A	GLU	3.3	Hydrophobic	166A	GLU	3.46
			Hydrogen Bond	189A	GLN	2.64	Hydrogen Bond	188A	ARG	1.7
			Hydrogen Bond	192A	GLN	3.19	Hydrogen Bond	189A	GLN	2.61
							Hydrogen Bond	192A	GLN	2.75
4c	-8.1	-8.9	Hydrophobic	41A	HIS	3.55	Hydrophobic	140A	PHE	3.75
			Hydrophobic	47A	GLU	3.31	Hydrophobic	165A	MET	3.83
			Hydrophobic	167A	LEU	3.36	Hydrophobic	166A	GLU	3.42
			Hydrophobic	168A	PRO	3.76	Hydrogen Bond	186A	VAL	2.07
			Hydrophobic	192A	GLN	3.36	Hydrogen Bond	188A	ARG	2.4
			Hydrogen Bond	47A	GLU	2.31	Hydrogen Bond	189A	GLN	2.67
			Hydrogen Bond	166A	GLU	3.24	Hydrogen Bond	192A	GLN	2.68
4d	-8.1	-5.8	Hydrophobic	140A	PHE	3.8	Hydrophobic	47A	GLU	3.32
			Hydrophobic	166A	GLU	3.35	Hydrophobic	168A	PRO	3.27
							Hydrogen Bond	1B	SER	2.02
							Hydrogen Bond	47A	GLU	3.16
							Hydrogen Bond	142A	ASN	3.07
4e	-7.4	-7.9	Hydrophobic	41A	HIS	3.57	Hydrophobic	41A	HIS	3.79
			Hydrophobic	47A	GLU	3.27	Hydrophobic	47A	GLU	3.34
			Hydrophobic	167A	LEU	3.56	Hydrophobic	192A	GLN	3.49
			Hydrophobic	168A	PRO	3.64	Hydrogen Bond	1B	SER	2
			Hydrophobic	192A	GLN	3.37	Hydrogen Bond	1B	SER	2.34
			Hydrogen Bond	47A	GLU	2.39	Hydrogen Bond	47A	GLU	2.73
CBMicro_ 032111 (Control)	-7	-7.2	Hydrophobic	47A	GLU	3.17	Hydrophobic	47A	GLU	3.16
			Hydrophobic	165A	MET	3.92	Hydrophobic	140A	PHE	3.9
			Hydrophobic	166A	GLU	3.68	Hydrophobic	166A	GLU	3.68
			Hydrophobic	189A	GLN	3.88	Hydrophobic	189A	GLN	3.86
			Hydrophobic	192A	GLN	3.95	Hydrophobic	192A	GLN	3.92
			Hydrogen Bond	189A	GLN	3.08	Hydrogen Bond	189A	GLN	3.11
			Hydrogen Bond	192A	GLN	2.4	Hydrogen Bond	192A	GLN	2.39
			Salt Bridges	41A	HIS	5.3				
CHEMBL 2235440 (Control)	-8	-8	Hydrophobic	25A	THR	3.76	Hydrophobic	25A	THR	3.76
			Hydrophobic	27A	LEU	3.83	Hydrophobic	27A	LEU	3.94
			Hydrophobic	140A	PHE	3.56	Hydrophobic	140A	PHE	3.65
			Hydrophobic	165A	MET	3.45	Hydrophobic	166A	GLU	3.62
			Hydrophobic	166A	GLU	3.44	Hydrogen Bond	142A	ASN	2.23
			Hydrogen Bond	142A	ASN	2.26	Hydrogen Bond	143A	GLY	2.75
			Hydrogen Bond	143A	GLY	2.61	Hydrogen Bond	189A	GLN	2.57
			Hydrogen Bond	189A	GLN	2.48	Hydrogen Bond	190A	THR	3.15
K36 (Control)	-6.8	-7.2	Hydrophobic	166A	GLU	3.8				
			Hydrophobic	168A	PRO	3.84				
			Hydrogen Bond	166A	GLU	2.05	Hydrogen Bond	166A	GLU	2.6
			Hydrogen Bond	166A	GLU	2.36	Hydrogen Bond	166A	GLU	2.14
			Hydrogen Bond	166A	GLU	2.23	Hydrogen Bond	189A	GLN	2.15
			Hydrogen Bond	188A	ARG	2.45	Hydrogen Bond	190A	THR	2.22
			Hydrogen Bond	189A	GLN	2.7	Hydrogen Bond	190A	THR	2.56
			Hydrogen Bond	190A	THR	2.17	Hydrogen Bond	192A	GLN	2.34
			Hydrogen Bond	190A	THR	3.28				
			Hydrogen Bond	192A	GLN	2.32				

O6K (Control)	-6.9	-7.3	Hydrophobic	27A	LEU	3.82	Hydrophobic	25A	THR	3.68
			Hydrophobic	166A	GLU	3.71	Hydrophobic	27A	LEU	3.64
			Hydrophobic	168A	PRO	3.39	Hydrophobic	47A	GLU	3.83
			Hydrogen Bond	47A	GLU	2.17	Hydrophobic	168A	PRO	3.43
			Hydrogen Bond	187A	ASP	3.2	Hydrophobic	189A	GLN	3.85
			Hydrogen Bond	189A	GLN	2.42	Hydrogen Bond	143A	GLY	2.99
			Hydrogen Bond	189A	GLN	2.14	Hydrogen Bond	166A	GLU	3.06
			Hydrogen Bond	192A	GLN	3.49	Hydrogen Bond	187A	ASP	3.19
							Hydrogen Bond	189A	GLN	2.18
							Hydrogen Bond	190A	THR	2.33
							Hydrogen Bond	192A	GLN	2.3
							Salt Bridges	47A	GLU	5.04

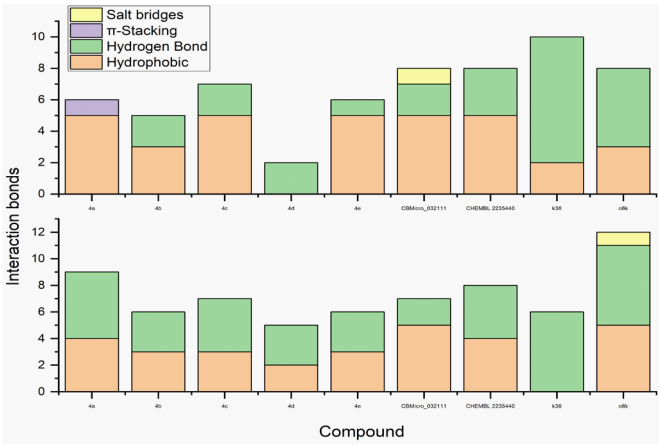

Figure 2: Number of interactions (Hydrogen bond, Hydrophobic interaction, Pi-staking and salt bridges) present in the 3C-like protease and ligand complex.

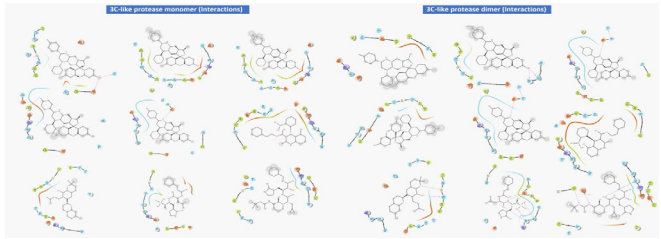

Figure 3: Molecular docking and interaction of 3C Like protease and 2-(4-chlorophenyl)-3',6'-dihydroxy-4-phenyl-8H-spiro[furo[3,4-g] quinoline-6,9'-xanthen]-8-one (**4**). **(A)** Aminoacid interaction in the active site between Dimer 3C like protease and synthesized molecule. **(B)** Aminoacid interaction in the active site between Monomer 3C like protease and synthesized molecule.

Conclusions

In conclusion, we have reported the synthesis of a novel class of quinoline. The most noteworthy aspect of this research is the development of an efficient and general route for the synthesis of the quinoline through a one-pot synthesis from aminofluorescein, benzaldehyde and phenylacetylene. This methodology of a one-pot three-component reaction in the synthesis of quinoline with substitution at the C-2 and C-4 positions appears attractive for the combinatorial synthesis of a quinoline library. Quinolines are potential antiviral molecules and in the present study, an attempt to find its potential against COVID 19 is been assed using *in silico* docking studies. This resulted in identifying the synthesized compound to be a potential inhibitor molecule against the 3C like protease both as monomer and dimer. Further *in vitro* and *in vivo* studies can help in finding the efficacy of the synthesized molecule as a potential antiviral agent.

Acknowledgement

M. R. acknowledges financial support from the DBT, New Delhi. The authors thank 'Sathyabama Institute of Science and Technology, Chennai, Tamilnadu, India' for providing infrastructure and instrumentation support to execute the research work.

References

1. Kouznetsov VV, Vargas Méndez LY, Puerto Galvis CE, Ortiz Villamizar MC. The direct C–H alkenylation of quinoline N -oxides as a suitable strategy for the synthesis of promising antiparasitic drugs. New J Chem. 2020; 44: 12–19.

2. Weyesa A, Mulugeta E. Recent advances in the synthesis of biologically and pharmaceutically active quinoline and its analogues: a review. RSC Adv. 2020; 10: 20784–20793.

3. Mekheimer RA, Al-Sheikh MA, Medrasi HY, Sadek KU. Advancements in the synthesis of fused tetracyclic quinoline derivatives. RSC Adv. 2020; 10: 19867–19935.

4. Lam KH, Lee KKH, Gambari R, Kok SHL, Kok TW, Chan ASC, et al. Anti-tumour and pharmacokinetics study of 2-Formyl-8-hydroxy-quinolinium chloride as Galipea longiflora alkaloid analogue. Phytomedicine. 2014; 21: 877-82.

5. Vincent MJ, Bergeron E, Benjannet S, Erickson BR, Rollin PE, et al. Chloroquine is a potent inhibitor of SARS coronavirus infection and spread. Virol J. 2005; 2: 69.

6. Lam KH, Gambari R, Lee KKH, Chen YX, Kok SHL, Wong RSM, et al. Preparation of 8-hydroxyquinoline derivatives as potential antibiotics against Staphylococcus aureus. Bioorg Med Chem Lett. 2014; 24: 367–370.

7. Vandekerckhove S, Tran HG, Desmet T, D'Hooghe M. Evaluation of (4-aminobutyloxy) quinolines as a novel class of antifungal agents. Bioorganic Med Chem Lett. 2013; 23: 4641-3.

8. Ratheesh M, Sindhu G, Helen A. Anti-inflammatory effect of quinoline alkaloid skimmianine isolated from Ruta graveolens L. Inflamm Res. 2013; 62: 367-76.

9. Kouznetsov V, Vargas Mendez L, Milena Leal S, Mora Cruz U, Andres Coronado C, et al., 2008. Target-Oriented Synthesis of Antiparasitic 2-Hetaryl Substituted Quinolines Based on Imino Diels-Alder Reactions. Lett Drug Des Discov. 2008; 4: 293-296.

10. Rolain JM, Colson P, Raoult D. Recycling of chloroquine and its hydroxyl analogue to face bacterial, fungal and viral infections in the 21st century. Int J Antimicrob Agents. 2007; 30: 297-308.

11. Zheng X, Wang L, Wang B, Miao K, Xiang K, et al. Discovery of Piperazinylquinoline Derivatives as Novel Respiratory Syncytial Virus Fusion Inhibitors. ACS Med Chem Lett. 2016; 7: 558-62.

12. Talamas FX, Abbot SC, Anand S, Brameld KA, Carter DS, Chen J, et al. Discovery of N-[4-[6-tert-butyl-5-methoxy-8-(6-methoxy-2-oxo-1 H -pyridin-3-yl)-3-quinolyl]phenyl]methanesulfonamide (RG7109), a potent inhibitor of the hepatitis C virus NS5B polymerase. J Med Chem. 2014; 57: 1914-1931.

13. Goodell JR, Puig-Basagoiti F, Forshey BM, Shi PY, Ferguson DM. Identification of compounds with anti-West Nile virus activity. J Med Chem. 2006.

14. Huang SH, Lien JC, Chen CJ, Liu YC, Wang CY, et al. Antiviral activity of a novel compound cw-33 against Japanese encephalitis virus through inhibiting intracellular calcium overload. Int J Mol Sci. 2016; 17: 1386.

15. Barbosa-Lima G, Moraes AM, Araújo A da S, da Silva ET, Freitas CS, et al. 2,8-bis(trifluoromethyl)quinoline analogs show improved anti-Zika virus activity, compared to mefloquine. Eur J Med Chem. 2017; 127: 334-340.

16. Kim J, Kim S, Kim D, Chang S. Ru-Catalyzed Deoxygenative Regioselective C8–H Arylation of Quinoline N -Oxides. J Org Chem. 2019; 84: 13150–13158.

17. You G, Xi D, Sun J, Hao L, Xia C. Transition-metal- and oxidant-free three-component reaction of quinoline: N -oxides, sodium metabisulfite and aryldiazonium tetrafluoroborates via a dual radical coupling process. Org Biomol Chem. 2019; 17: 9479-9488.

18. Upadhyay A, Chandrakar P, Gupta S, Parmar N, Singh SK, et al. Synthesis, Biological Evaluation, Structure–Activity Relationship, and Mechanism of Action Studies of Quinoline–Metronidazole Derivatives Against Experimental Visceral Leishmaniasis. J Med Chem. 2019; 62: 5655–5671.

19. Tarnow P, Zordick C, Bottke A, Fischer B, Kuhne F, et al. Characterization of Quinoline Yellow Dyes As Transient Aryl Hydrocarbon Receptor Agonists. Chem Res Toxicol. 2020; 33: 742–750.

20. Ko MS, Kurapati S, Jo Y, Cho B, Cho DG. Tuned Al3+ selectivity and π-extended properties of di-2-picolylamine-substituted quinoline-based tolan. Tetrahedron Lett. 2020; 61: 151808.

21. Vuong H, Stentzel MR, Klumpp DA. Superacid-promoted synthesis of quinoline derivatives. Tetrahedron Lett. 2020; 61: 151630.

22. Rajasekar M, Mohan Das T. Synthesis and antioxidant properties of novel fluorescein-based quinoline glycoconjugates. J Carbohydr Chem. 2014; 137-151.

23. Shi Y, Zhang X, Mu K, Peng C, Zhu Z, Wang X, et al. D3Targets-2019-nCoV: a webserver for predicting drug targets and for multi-target and multi-site based virtual screening against COVID-19. Acta Pharm. Sin B. 2020; 10: 1239-1248.

24. Trott O, Olson AJ. AutoDock Vina: improving the speed and accuracy of docking with a new scoring function, efficient optimization, and multithreading. J Comput Chem. 2010; 31: 455–61.